行政院國家科學委員會專題研究計畫 期末報告

內皮素 A 型受體拮抗劑配合運動治療對睡眠呼吸終止症誘發心臟細胞凋亡的療效探討(第 3 年)

計 畫 類 別 ：個別型
計 畫 編 號 ：NSC 98-2314-B-040-001-MY3
執 行 期 間 ：100 年 08 月 01 日至 101 年 12 月 31 日
執 行 單 位 ：中山醫學大學醫學研究所

計 畫 主 持 人：丁化
共 同 主 持 人：李信達

報 告 附 件 ：出席國際會議研究心得報告及發表論文

公 開 資 訊 ：本計畫涉及專利或其他智慧財產權，1 年後可公開查詢

中 華 民 國 102 年 06 月 18 日

中 文 摘 要 ： 已被證實與消耗果糖代謝綜合徵的發展，而心肌病的變化和心肌細胞凋亡的膳食攝入高果糖尚未闡明。這項研究的目的是評估高果糖的影響對心肌細胞凋亡和生存途徑。 36Wistar大鼠隨機分為對照組（CON)標準的飼料，果糖誘發代謝綜合徵組（FIMS），獲得了50％的果糖含量為13週的飲食。病理組織學分析，TUNEL法和Western印跡進行切除心中兩組。血壓，血糖，胰島素，甘油三酯和膽固醇水平顯著增加在FIMS組，與CON組相比。異常的心肌結構，間隙擴大和增加心臟TUNEL陽性細胞凋亡，觀察在FIMS組。 TNF-腫瘤壞死因子受體1，Fas配體，Fas受體，FADD，caspase-3的活化，8個蛋白水平（FAS途徑）和Bax蛋白表達，比克，Bax/Bcl-2的，比克/ Bcl-xL的，胞漿內細胞色素c和活化的caspase-3和9個蛋白水平（線粒體途徑）FIMS組與CON組相比增加。 IGFI，IGFI-R，P-PI3K，p-Akt蛋白，Bcl-2和Bcl-xL的蛋白水平（生存途徑）均顯著下降FIMS組與CON組相比。高果糖攝入血壓升高和血糖水平，而且，高果糖飲食心臟FAS依賴性和線粒體依賴性凋亡通路激活和抑制的生存途徑，這可能提供一個發展與代謝綜合徵患者心臟衰竭的可能機制。

中文關鍵詞： Fas受體細胞凋亡；果糖；；心臟；代謝綜合徵，腫瘤壞死因子-α

英 文 摘 要 ： Consumption of fructose has been linked to the development of metabolic syndrome, whereas the cardiomyopathic changes and cardiac apoptosis of dietary high-fructose intake have not yet been clarified. The purpose of this study was to evaluate the effects of high-fructose on cardiac apoptotic and survival pathways. Thirty-two Wistar rats were randomly divided into a control group (CON), which received a standard chow diet, and a fructose-induced metabolic syndrome group (FIMS), which received a 50% fructose-content diet for 13 weeks.
Histopathological analysis, TUNEL assays and Western blotting were performed on the excised hearts from both groups. The blood pressure, glucose, insulin, triglyceride and cholesterol levels were significantly increased in the FIMS group, compared with the CON group. The abnormal myocardial architecture, enlarged interstitial space and

increased cardiac TUNEL-positive apoptotic cells were observed in the FIMS group. The TNF-a, TNF receptor 1, Fas ligand, Fas receptor, FADD, and activated caspase-3 and 8 protein levels (Fas pathway) and the Bax, Bak, Bax/Bcl-2, Bak/Bcl-xL, cytosolic cytochrome c, and activated caspase-3 and nine protein levels (mitochondria pathway) were increased in the FIMS group compared with those in the CON group. The IGFI, IGFI-R, p-PI3K, p-Akt, Bcl-2 and Bcl-xL protein levels (survival pathway) were all significantly decreased in the FIMS group compared with those in the CON group. High-fructose intake elevated blood pressure and glucose levels; moreover, high-fructose diet activated cardiac Fas-dependent and mitochondria-dependent apoptotic pathways and suppressed the survival pathway, which might provide one possible mechanism for developing heart failure in patients with metabolic syndrome.

英文關鍵詞： Apoptosis; Fructose; Fas receptor; Heart; Metabolic syndrome; TNF-alpha

SPi	Journal Code				Article ID				Dispatch: 25.04.13	CE:
	C	B	F		2	9	8	2	No. of Pages: 9	ME:

CELL BIOCHEMISTRY AND FUNCTION
Cell Biochem Funct (2013)
Published online in Wiley Online Library
(wileyonlinelibrary.com) **DOI**: 10.1002/cbf.2982

Activated apoptotic and anti-survival effects in ~~fructose-induced metabolic syndrome~~ rat hearts

Shiu-Min Cheng[1], Yu-Jung Cheng[2], Liang-Yi Wu[3], Chia-Hua Kuo[2,4], Yi-Shin Lee[2], Ming-Che Wu[5], Chih-Yang Huang[6,7,8], Hua Tin[5,9,†] and Shin-Da Lee[2,10]*,†

[1]*Department of Psychology, Asia University, Taichung, Taiwan*
[2]*Department of Physical Therapy, Graduate Institute of Rehabilitation Science, China Medical University, Taichung, Taiwan*
[3]*Department of Bioscience Technology, Chung Yuan Christian University, Taoyuan, Taiwan*
[4]*~~Laboratory of Exercise Biochemistry, Taipei Physical Education College~~, Taipei, Taiwan*
[5]*Department of Physical Medicine and Rehabilitation, Chung-Shan Medical University Hospital, Chung-Shan Medical University, Taichung, Taiwan*
[6]*School of Chinese Medicine, College of Chinese Medicine, China Medical University, Taichung, Taiwan*
[7]*Graduate Institute of Basic Medical Science, China Medical University, Taichung, Taiwan*
[8]*Department of Health and Nutrition Biotechnology, Asia University, Taichung, Taiwan*
[9]*~~School~~ of Medicine, Chung-Shan Medical University, Taichung, Taiwan*
[10]*Department of Healthcare Administration, Asia University, Taichung, Taiwan*

Consumption of fructose has been linked to the development of metabolic syndrome, whereas the cardiomyopathic changes and cardiac apoptosis of dietary high-fructose intake have not yet been clarified. The purpose of this study was to evaluate the effects of high-fructose on cardiac apoptotic and survival pathways. Thirty-two Wistar rats were randomly divided into a control group (CON), which received a standard chow diet, and a fructose-induced metabolic syndrome group (FIMS), which received a 50% fructose-content diet for 13 weeks. Histopathological analysis, TUNEL assays and Western blotting were performed on the excised hearts from both groups. The blood pressure, glucose, insulin, triglyceride and cholesterol levels were significantly increased in the FIMS group, compared with the CON group. The abnormal myocardial architecture, enlarged interstitial space and increased cardiac TUNEL-positive apoptotic cells were observed in the FIMS group. The TNF-α, TNF receptor 1, Fas ligand, Fas receptor, FADD, and activated caspase-3 and 8 protein levels (Fas pathway) and the Bax, Bak, Bax/Bcl-2, Bak/Bcl-xL, cytosolic cytochrome *c*, and activated caspase-3 and nine protein levels (mitochondria pathway) were increased in the FIMS group compared with those in the CON group. The IGFI, IGFI-R, p-PI3K, p-Akt, Bcl-2 and Bcl-xL protein levels (survival pathway) were all significantly decreased in the FIMS group compared with those in the CON group. High-fructose intake elevated blood pressure and glucose levels; moreover, high-fructose diet activated cardiac Fas-dependent and mitochondria-dependent apoptotic pathways and suppressed the survival pathway, which might provide one possible mechanism for developing heart failure in patients with metabolic syndrome. Copyright © 2013 John Wiley & Sons, Ltd.

KEY WORDS—Apoptosis; Fructose; Fas receptor; Heart; Metabolic syndrome; TNF-alpha

INTRODUCTION

Metabolic syndrome is a cluster of symptoms including central obesity, insulin resistance, hyperglycemia, dyslipidemia and hypertension, all of which are risk factors for the development of obesity, type 2 diabetes and cardiovascular disease (CVD).[1–4] The high prevalence of metabolic syndrome has significant public health implications because of the sixfold risk of developing type 2 diabetes, twofold increased risk of prevalence of coronary heart disease and threefold increased risk of mortality attributable to coronary heart disease.[5] Most studies regarding metabolic syndrome show that it may lead to deteriorated cardiac geometry and function of CVD and heart failure.[2–5] Cellular apoptosis in terminally differentiated cardiomyocytes is a very critical pathological mechanism in the cause of heart failure, whereas, on the other hand, the process of apoptotic interruption may be allowed to develop a novel strategy to reverse or attenuate heart failure.[6,7] Moreover, cardiac apoptosis has been found in obesity, diabetes and hypertension.[7–10]

Apoptosis, a physiological program of cellular death, may contribute to many cardiac disorders.[11,12] The occurrence of apoptosis has been reported to contribute to the loss of cardiomyocytes in cardiomyopathy and is recognized as a predictor of adverse outcomes in subjects with cardiac diseases or heart failure.[6] The 'extrinsic' Fas ligand or tumor necrosis factor-alpha (TNF-α)–dependent (type I) apoptotic

*Correspondence to: Shin-Da Lee, Department of Physical Therapy, Graduate Institute of Rehabilitation Science, China Medical University, 91 Hsueh-Shih Road, Taichung, Taichung, 40202, Taiwan. E-mail: shinda@mail.cmu.edu.tw
†Share equal contribution.

Received 26 December 2012
Revised 8 April 2013
Accepted 9 April 2013

pathway is believed to be one of the major pathways directly to trigger cardiac apoptosis.[12–14] This pathway is often initiated by binding the Fas ligand to the Fas death receptor or by binding the TNF-α to TNF receptor 1 (TNFR1), which results in the clustering of receptors and the initiation of an extrinsic pathway.[13] Fas ligand and Fas receptor or TNF-α and TNFR1 complex are known to lead to the formation of a death-inducing signal complex starting with the recruitment of the Fas-associated death domain (FADD) of the adaptor protein.[13] FADD is known to function as a common signaling conduit in Fas and TNF-α–mediated apoptosis.[15] FADD recruits and aggregates the pro-caspase-8 and leads to its activation of caspase-8.[14] The activated caspase-8 cleaves pro-caspase-3, which then undergoes autocatalysis to form active caspase-3, a principle effector caspase of apoptosis.[16]

The 'intrinsic' mitochondria-dependent (type II) apoptotic pathway starts from within the cell, resulting in the release of a number of pro-apoptotic factors from the intermembrane space of mitochondria.[13,14] The mitochondria is the main site of action for members of the apoptosis-regulating protein family exemplified by Bcl-2 family, such as Bax (Bcl-2-associated X protein) and Bak (pro-apoptotic molecular).[13] Commitment to apoptosis is typically governed by opposing factions of the Bcl-2 family, including pro-apoptotic versus anti-apoptotic family members.[17] Pro-apoptotic and pro-survival Bcl-2 family members can homodimerize or heterodimerize to each other and appear to interact with and neutralize each other so that the relative balance of these effectors strongly influences cytochrome *c* release.[18] Bcl-2 and Bcl-xL, pro-survival proteins prevent cytochrome *c* release, whereas Bax and Bak enhance cytochrome *c* release from the mitochondria.[13] When cytochrome *c* is released from mitochondria into the cytosol, it is responsible for activating caspase-9, which further activates caspase-3 and executes the apoptotic program.[19] Cardiac Fas-dependent and mitochondria-dependent apoptotic pathways are involved in many pathologic conditions such as hypoxic stress, hypertension and obesity.[20–24] However, it is unclear whether cardiac Fas-dependent and mitochondria-dependent apoptotic pathways mediate metabolic syndrome-related cardiac apoptosis.

Insulin-like growth factor I (IGFI) signaling is reported to contribute to the modulation of survival responses in cardiac tissues. Phosphatidylinositol 3-kinase (PI3K) and protein kinase B (Akt) are key signaling factors in insulin and IGFI-receptor (IGFI-R).[25–28] Impaired IGFI signaling may contribute, at least partially, to the development of diabetes and the pathology of cardiac apoptosis in diabetic animals and humans.[8,29] Akt is one of the major upstream signal proteins of the Bcl-2 family, and phosphorylated Akt (p-Akt) appears to promote the pro-survival pathway.[30] However, the cardiac IGFI-related survival pathway in the metabolic syndrome animal model has not yet been reported.

A well-known experimental model of metabolic syndrome is induced by feeding rats with a high-fructose diet. This model induces weight gain, hypertension, hyperinsulinemia, hyperlipidemia and insulin resistance.[31,32] The current study was undertaken to understand the effects of high-fructose on the cardiac Fas-dependent apoptotic (TNF-α, TNFR1, Fas ligand, Fas receptor, FADD, activated caspase-8, and activated caspase-3), mitochondria-dependent apoptotic (Bax, Bak, cytosolic cytochrome *c*, activated caspase-9 and activated caspase-3) and survival (IGFI, IGFI-R, p-PI3K, p-Akt, Bcl-2 and Bcl-xL) pathways in rats. We hypothesized that fructose-induced metabolic syndrome rats may be predisposed to more activated cardiac Fas-dependent and mitochondria-dependent apoptotic pathways, as well as suppressed cardiac IGFI-related survival and Bcl-2 family associated pro-survival pathways.

METHODS

Animals and induction of metabolic syndrome

Thirty-two male Wistar sixteen-week-old rats were obtained from the National Laboratory Animal Center, Taiwan. Ambient temperature was maintained at 25 °C, and the animals were kept on an artificial 12-h light–dark cycle. The light period beginning at 700 h. Rats were fed with a standard Purina chow diet (#5001, Purina, St. Louis, MO, USA; based on dry weight, composed of 23% protein, 56% carbohydrate, 4.5% fat, and 6% fiber) and water *ad libitum*. All experimental procedures were performed according to the NIH Guide for the Care and Use of Laboratory Animals, and all protocols were approved by the Institutional Animal Care and Use Committee of China Medical University, Taichung, Taiwan.

All animals were allowed to adapt to the environment for one week after their arrival before the experiment started. The animals were fed with standard Purina chow diet for 5 days, and no statistical differences in body weight, blood pressure, blood glucose, insulin, triglyceride, and cholesterol were found before the beginning of the experiment. The glucose level was detected by Accu Soft (Roche, Indianapolis, IN, USA) test strips. Systolic, diastolic and mean arterial blood pressure were measured with an automated tail-cuff system (29SSP; IITC/Life Science Instruments). The average of five consecutive readings for accurate measurement was used for blood pressure.

The animals were divided into a control group (CON, $n = 16$), which received standard Purina chow diet and a fructose-induced metabolic syndrome group (FIMS, $n = 16$), which received a high fructose-content diet (composed of 21% protein, 50% fructose, 5% fat and 8% fiber as a percentage of total calories) . All groups were followed for 13 weeks. Eight rats from each group were used for western blot analysis, and the remaining eight rats from each group were used for pathological staining.

Blood collection and tissue extraction

At the end of the experiment, all animals were sacrificed after overnight fasting, trunk blood samples were collected in heparinized tubes. Blood samples were centrifuged at 2000 *g* for 10 min at 4 °C; then, the plasma was collected and stored at −20 °C until assayed for insulin, triglyceride and cholesterol. Cardiac tissue extracts were obtained by homogenizing the left ventricle samples in a lysis buffer

(20 mM of Tris, 2 mM of EDTA, 50 mM of 2-mercaptoethanol, 10% glycerol, pH 7·4, proteinase inhibitor (Roche), phosphatase inhibitor cocktail (Sigma Chemical Co., Louis, MO, USA)) at a ratio of 100 mg tissue per 1 ml buffer for 1 min. The homogenates were placed on ice for 10 min and then centrifuged at 12 000 *g* for 40 min, twice. The supernatant was collected and stored at −70 °C for further investigations.

Cardiac characteristics and heart weight

The hearts of the rats from both groups were analysed using heart weight index and Western blotting. The hearts were excised and cleaned with phosphate-buffered saline (PBS). The left ventricles were separated and weighed. The ratios of the whole heart weight (WHW) to body weight (BW), the ratios of the left ventricular weight (LVW) to BW, the ratios of the LVW to WHW, the ratios of the WHW to tibia length and the ratios of the LVW to tibia length were calculated.

Biochemical assays

Plasma insulin concentrations were measured using a commercial ELISA kit (Mercodia, Uppsala, Sweden). Plasma triglyceride and cholesterol concentrations were assayed with commercial kits (E. Merck, Darmstadt, Germany) by enzymatic photocolorimetric methods.

Hematoxylin–eosin staining

The hearts from rats were excised and soaked in formalin, dehydrated through graded alcohols and embedded in paraffin wax. The 3-μm thick paraffin sections were cut from the paraffin-embedded tissue blocks. The tissue sections were deparaffinized by immersing in xylene and rehydrated. They were passed through a series of graded alcohols (100%, 95% and 75%), for 15 min of each. The slides were then dyed with hematoxylin for 5–10 min, followed by washing with tap water for 10–20 min. The slides were then soaked in mild warm water until it turned bright violent before putting it into eosin solution for 3–5 min. After gently rinsing with water, each slide was soaked in 85% alcohol and 100% alcohol I and alcohol II for 15 min each. The final step was to soak in xylene I and xylene II. Photomicrographs were obtained using Zeiss Axiophot microscopes. The slices were measured by the software 'Adobe Photoshop CS3'. The mean number of myocardial interstitial spaces was quantified for at least 5–6 separate fields × 2 slides × 3 regions of each left ventricle (upper, middle and lower) excised from the rats' hearts. All counts were performed by at least two independent individuals in a blinded manner.[8]

DAPI staining and terminal deoxynucleotide transferase-mediated dUTP nick end labeling

The hearts were excised, soaked in formalin, dehydrated through graded alcohols and embedded in paraffin wax. Sections 3 μm thick were prepared from these paraffin-embedded tissue blocks. The sections were deparaffinized by immersing in xylene, rehydrated and incubated in phosphate-buffered saline with 2% H_2O_2 to inactivate endogenous peroxidases. Next, the sections were incubated with proteinase K (20 $\mu g \cdot ml^{-1}$), washed in phosphate-buffered saline and incubated with terminal deoxynucleotidyl transferase and fluorescein isothiocyanate-dUTP for 1 h at 37 °C using an apoptosis detection kit (Roche). After washing twice in PBS, the sections were stained with 4', 6-diamidine-2-phenylindole dihydrochloride (DAPI, Sigma Chemical Co.) for 5 min to allow the cell nucleus to be detected by UV light microscopic observations (blue). TUNEL-positive nuclei (fragmented DNA) fluoresce bright green at 450–500 nm, whereas DAPI-positive nuclei (intact DNA) fluoresce blue at 360 nm. The mean number of TUNEL-positive cells were counted for at least 5–6 separate fields × 2 slides × 3 regions of each left ventricle (upper, middle and lower) excised from the rats' hearts. All counts were performed by at least two independent individuals in a blinded manner.

Separation of cytosolic and mitochondrial fractions

To detect cytosolic cytochrome c, tissues were suspended in a buffer (50mM Tris (pH 7·5), 0·5 M NaCl, 1·0 mM of EDTA (pH 7·5), 10% glycerol and proteinase inhibitor cocktail tablet (Roche) for 3 min on ice), homogenized by 40 strokes in a Dounce homogenizer, and centrifuged at 12 000 *g* for 15 min. The supernatant was the cytosol fraction, and the pellet was resuspended in lysis buffer as the membrane fraction.

Electrophoresis and Western blot

Protein concentration of cardiac tissue extracts was determined by the Lowry protein assay. Protein samples (40 $\mu g\,lane^{-1}$) were separated on a 10% SDS polyacrylamide gel electrophoresis (SDS-PAGE) with a constant voltage of 75 V. Electrophoresed proteins were transferred to a polyvinylidene difluoride (PVDF) membrane (0·45 μm pore size, Millipore, Bedford, MA, USA) with a transfer apparatus (Bio-Rad Laboratories Inc., Berkeley, CA, USA). PVDF membranes were incubated in 5% milk in TBS buffer. Primary antibodies including TNF-α, TNFR1, Fas ligand, Fas receptor, FADD, Bax, Bak, Bcl-2, Bcl-xL, caspase-3, caspase-8, caspase-9, cytochrome *c*, IGFI, IGFI-R, p-PI3K (Santa Cruz Biotechnology, Santa Cruz, CA, USA), p-Akt (Cell Signaling Technology Inc., Beverly, MA, USA) and α-tubulin (Neo Markers, Fremont, CA, USA) were diluted to 1:500 in antibody binding buffer overnight at 4 °C. The immunoblots were washed three times in TBS buffer for 10 min and then immersed in a second antibody solution containing goat anti-mouse IgG-HRP, goat anti-rabbit IgG-HRP, or donkey anti goat IgG-HRP (Santa Cruz Biotechnology) for 1 h and diluted 500-fold in TBS buffer. The immunoblots were then washed three times in TBS buffer for 10 min. The immunoblotted proteins were visualized using an enhanced chemiluminescence ECL Western blotting luminal reagent (Santa Cruz Biotechnology) and quantified using a Fujifilm LAS-3000 chemiluminescence detection system (Fujifilm, Tokyo,

Japan). Densitometric analyses of immunoblots were performed with an AlphaImager 2200 digital imaging system (Digital Imaging System, San Leandro, CA, USA).

Table 1. Measurements of subjects

	CON	FIMS
Number of animals	8	8
Body weight (BW), g	539 ± 44	570 ± 64
Heart weight index		
Whole heart weight (WHW), g	1·57 ±0·15	1·65 ± 0·20
Left ventricle weight (LVW), g	1·19 ± 0·11	1·31 ± 0·16
WHW/BW ($\times 10^3$)	2·83 ± 0·22	2·82 ± 0·12
LVW/BW ($\times 10^3$)	2·15 ± 0·22	2·28 ± 0·23
LVW/WHW	0·76 ± 0·03	0·80 ± 0·06
WHW/tibia length ($\times 10$), g mm^{-1}	0·32 ± 0·02	0·34 ± 0·06
Blood pressure		
SBP, mmHg	110 ± 5	129 ± 8*
DBP, mmHg	78 ± 9	99 ± 6*
MBP, mmHg	89 ± 4	109 ± 7*
Biochemical parameters		
Glucose, mg dl^{-1}	110·7 ± 4·3	124 ± 5·7*
Insulin, ng dl^{-1}	0·22 ± 0·08	0·59 ± 0·15*
Triglyceride, mg dl^{-1}	76·1 ± 15·4	139·8 ± 19·3*
Cholesterol, mg dl^{-1}	62·6 ± 9·1	81·3 ± 10·8*

Values are means ± SD body weight, heart weight index, systolic blood pressure (SBP), diastolic blood pressure (DBP), mean arterial blood pressure (MBP) and biochemical parameters in the control group (CON), which received a standard Purina chow diet and fructose-induced metabolic syndrome group (FIMS), which received a 50% fructose-content diet for 13 weeks.
*$P < 0·05$, significant difference versus the CON group.

Statistical analysis

All data for body weight, heart weight index, blood pressure, biochemical parameters, protein levels, and percentage of TUNEL-positive cells were compared between the CON and FIMS groups using Student's *t*-test for two independent samples. In all cases, a difference at $P < 0·05$ was considered statistically significant.

RESULTS

Cardiac characteristics, blood pressure and biochemical parameters

The index of whole heart weight (WHW), left ventricular weight (LVW), WHW/body weight (BW), LVW/BW, LVW/WHW and WHW/tibia length were similar in the CON and FIMS groups. The systolic blood pressure (SBP), diastolic blood pressure (DBP) and mean arterial blood pressure (MBP) in the FIMS group were higher than those in the CON group ($P < 0·05$), as shown in Table 1. The concentrations of blood glucose, plasma insulin, triglyceride and cholesterol in the FIMS group were higher than those in the CON group (Table 1). T1

Cardiac histopathological changes

To investigate changes of cardiac architecture in fructose-induced metabolic syndrome, we performed a histopathological

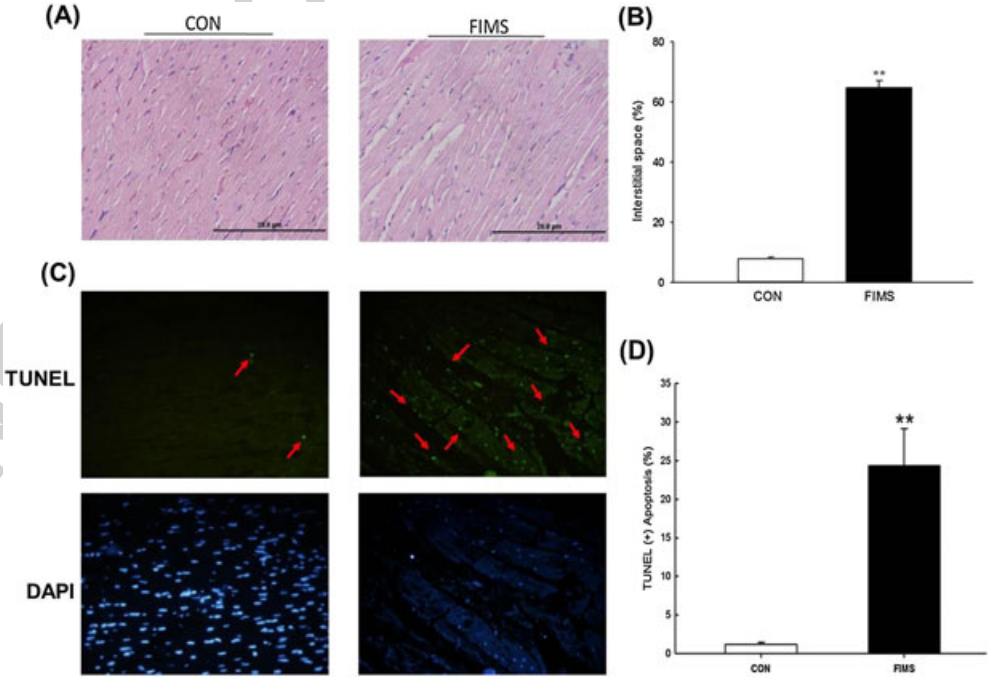

Figure 1. **(A)** Representative histopathological analysis of cardiac sections from the left ventricles with H&E staining in the control group (CON), which received a standard Purina chow diet and the fructose-induced metabolic syndrome group (FIMS), which received a 50% fructose-content diet for 13 weeks. The images of cardiac architecture were magnified 400 times. (B) Bars represent the percentage of myocardial interstitial space to total area. (C) Representative stained apoptotic cells of cardiac sections from the left ventricle in the CON group and the FIMS group as measured by staining with TUNEL (upper panels, green spots) and DAPI assay with dark background (lower panels, blue sports). The images of cardiac architecture were magnified 400 times. (D) Bars represent the percentage of TUNEL-positive cells relative to total DAPI cells. All bars indicate mean values ± SD ($n = 8$ in each group). **$P < 0·01$, significant difference from the CON group

analysis of ventricular tissue stained with hematoxylin and eosin (H&E). The ventricular myocardium in the CON group showed normal architecture with normal interstitial space, but the abnormal myocardial architecture and the increased interstitial spaces were observed in the FIMS group (Figure 1A and 1B). **F1**

TUNEL-positive apoptotic cells of cardiac tissue

To reconfirm the apoptotic activity in fructose-induced metabolic syndrome, we examined the apoptotic cardiac cells in the excised hearts of the CON and FIMS groups by TUNEL assay. We observed that the left ventricles stained with TUNEL assay showed significantly increased TUNEL-positive cardiac cells in the FIMS group compared with the CON group, at 400× magnification images (Figure 1C and D).

Upstream components of cardiac Fas-dependent apoptotic pathways

To understand the changes to the cardiac Fas-dependent apoptotic pathway in fructose-induced metabolic syndrome, the protein levels of TNF-α, TNFR1, Fas ligand, Fas receptor and FADD were measured in the excised hearts of the CON and FIMS groups by Western blotting (Figure 2A). **F2**

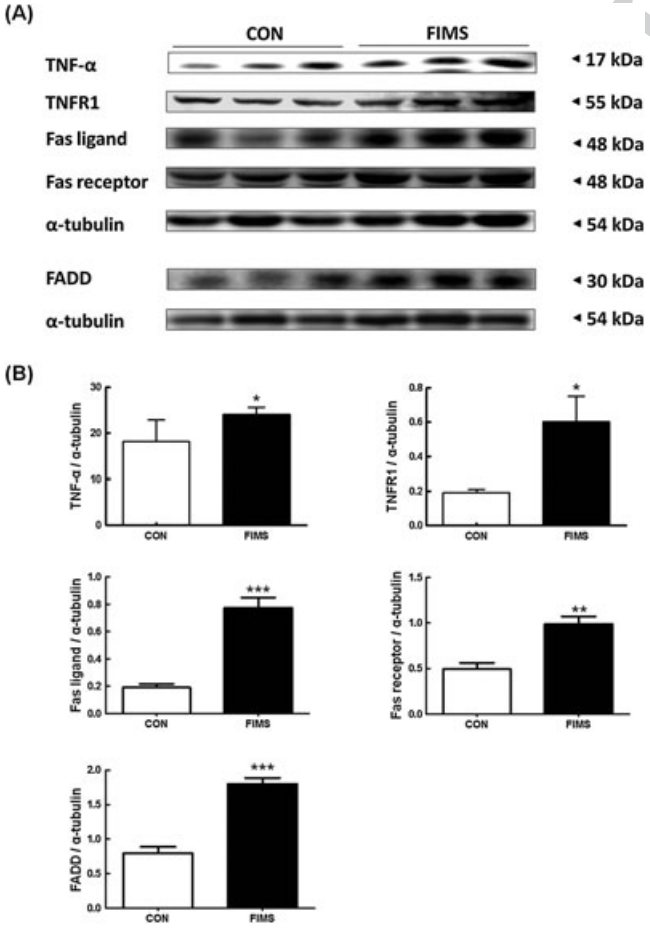

Figure 2. (A) Western blot analysis of the representative protein products of TNF-α, TNFR1, Fas ligand, Fas receptor and FADD extracted from the left ventricles of excised hearts in the control group (CON), which received a standard Purina chow diet and the fructose-induced metabolic syndrome group (FIMS), which received a 50% fructose-content diet for 13 weeks. (B) Bars represent the relative protein quantification of TNF-α, TNFR1, Fas ligand, Fas receptor and FADD on the basis of α-tubulin. All bars indicate mean values ± SD ($n = 8$ in each group). $^{*}P < 0{\cdot}05$, $^{**}P < 0{\cdot}01$, $^{***}P < 0{\cdot}001$ significant difference from the CON group

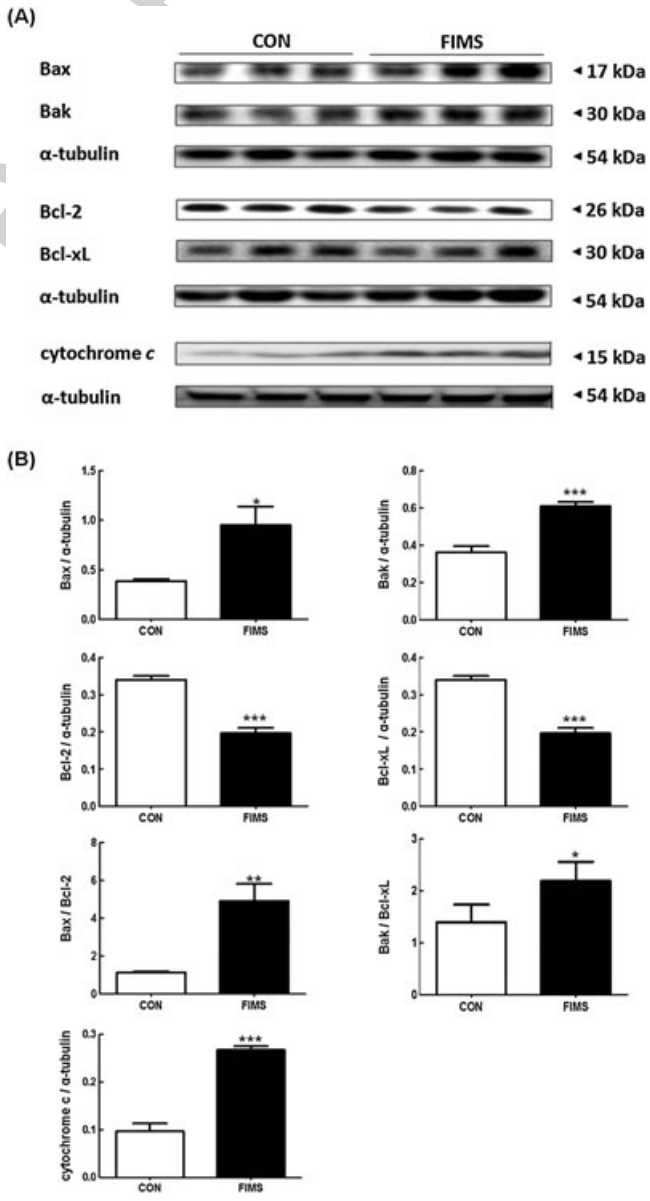

Figure 3. (A) Western blot analysis of the representative protein products Bax, Bak, Bcl-2, Bcl-xL and cytosolic cytochrome *c* extracted from the left ventricles of excised hearts in the control group (CON), which received a standard Purina chow diet and the fructose-induced metabolic syndrome group (FIMS), which received a 50% fructose-content diet for 13 weeks. (B) Bars represent the relative protein quantifications of Bax, Bak, Bcl-2, Bcl-xL and cytosolic cytochrome *c* on the basis of α-tubulin, All bars indicate mean values ± SD ($n = 8$ in each group). $^{*}P < 0{\cdot}05$, $^{**}P < 0{\cdot}01$, $^{***}P < 0{\cdot}001$, significant difference from the CON group

The protein levels of TNF-α, TNFR1, Fas ligand, Fas receptor and FADD in the FIMS group were significantly higher than those in the CON group (Figure 2B).

Upstream components of cardiac mitochondria-dependent apoptotic and Bcl-2 family–associated pro-survival pathways

To understand the changes of cardiac mitochondria-dependent apoptotic and Bcl-2 family associated pro-survival pathways in fructose-induced metabolic syndrome, the protein levels of Bax, Bak, Bcl-2, Bcl-xL and cytosolic cytochrome *c* were measured in the excised hearts of the CON and FIMS groups using Western blotting (Figure 3A). The protein levels of Bax, Bak, cytochrome *c*, Bax/Bcl-2 and Bak/Bcl-xL in the FIMS group were significantly increased compared with those in the CON group (Figure 4B). In addition, the protein levels of Bcl-2 and Bcl-xL were significantly decreased in the FIMS group compared with those in the CON group (Figure 3B).

Downstream components of cardiac Fas-dependent and mitochondria-dependent apoptotic pathways

To identify the downstream components of cardiac Fas (caspase-8 and 3) and mitochondria (caspase-9 and 3)–dependent apoptotic pathways in fructose-induced metabolic syndrome, the protein levels of activated caspase-8, 9 and 3 were measured in the excised hearts of the CON and FIMS groups using Western blotting (Figure 4A). The protein levels of caspase-8, 9 and 3 were significantly increased in the FIMS group compared with those in the CON group (Figure 4B).

Cardiac survival pathway

To identify the cardiac IGFI-R-related PI3K-Akt survival pathway in fructose-induced metabolic syndrome, the protein levels of IGFI, IGFI-R, p-PI3K, and p-Akt were measured in the excised hearts of the CON and FIMS groups using Western blotting (Figure 5A). The protein levels of IGFI, IGFI-R, p-PI3K and p-Akt were significantly decreased in the FIMS group compared with those in the CON group (Figure 5B).

DISCUSSION

Our main new findings can be summarized as follows: (1) The blood pressure, glucose, insulin, triglyceride and cholesterol levels were significantly increased in the fructose (50%)–fed rats, a metabolic syndrome model, relative to the non-fructose fed rats. (2) Abnormal myocardial architecture, enlarged interstitial space and increased cardiac TUNEL-positive apoptotic cells were observed in the fructose-induced metabolic syndrome but not in the non-metabolic syndrome. (3) The cardiac Fas-dependent apoptotic proteins

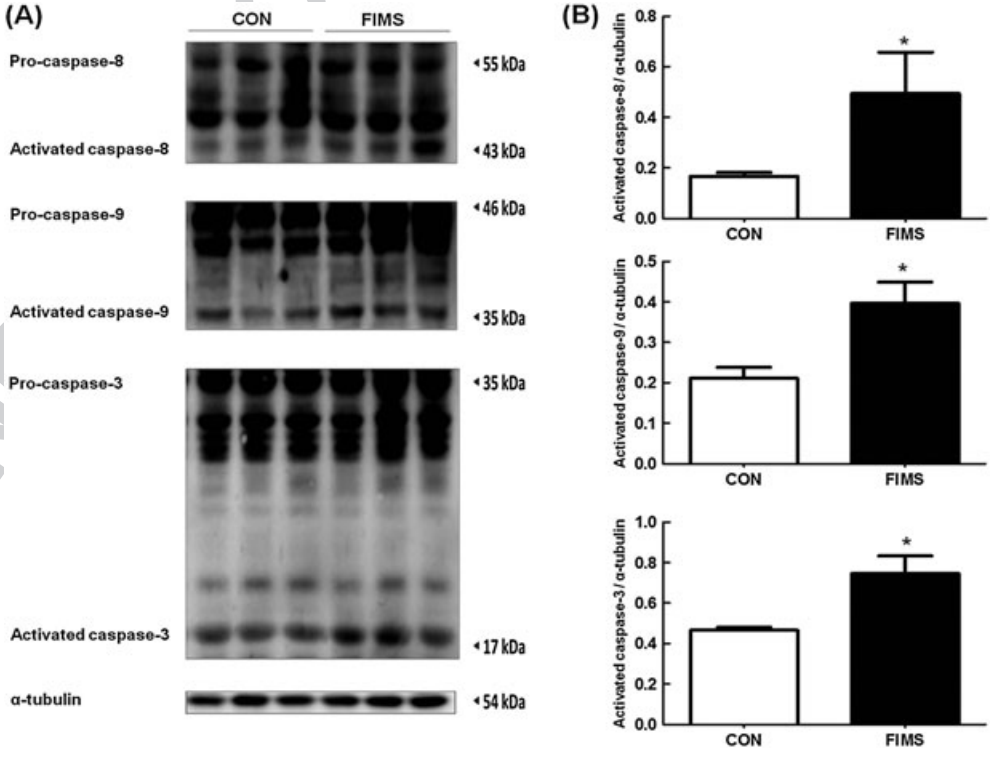

Figure 4. (A) Western blot analysis of the representative protein products of caspase-8, caspase-9 and caspase-3 extracted from the left ventricle in control group (CON), which received a standard Purina chow diet and fructose-induced metabolic syndrome group (FIMS), which received a 50% fructose-content diet for 13 weeks. (B–D) Bars represent the relative protein quantification of caspase-8, caspase-9 and caspase-3 on the basis of α-tubulin. All bars indicate mean values ± SD ($n = 8$ in each group). Bars present the statistic result. $^*P < 0{\cdot}05$, significant difference from the CON group

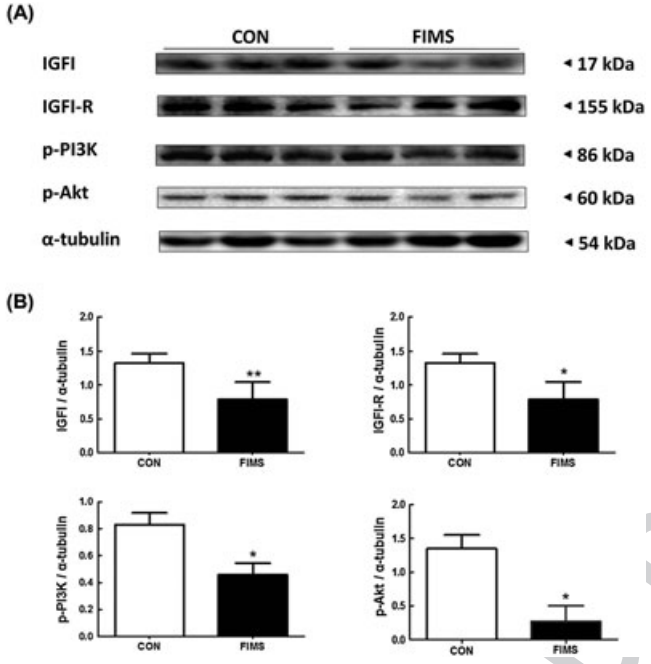

Figure 5. (A) Western blot analysis of the representative protein products of IGFI, IGFI-R, p-PI3K and p-Akt extracted from the left ventricles of excised hearts in the control group (CON), which received a standard Purina chow diet and the fructose-induced metabolic syndrome group (FIMS), which received a 50% fructose-content diet for 13 weeks. (B) Bars represent the relative protein quantification of IGFI, IGFI-R, p-PI3K and p-Akt on the basis of α-tubulin. All bars indicate mean values ± SD ($n = 8$ in each group). $^{*}P < 0{\cdot}05$, $^{**}P < 0{\cdot}01$, significant difference from the CON group

(TNF-α, TNFR1, Fas ligand, Fas receptor, FADD, activated caspase-8 and activated caspase-3) in the fructose-induced metabolic syndrome were significantly increased compared to the non-metabolic syndrome. (4) The cardiac mitochondria-dependent apoptotic proteins (Bax, Bak, Bax/Bcl-2, Bak/Bcl-xL, cytosolic cytochrome *c*, activated caspase-9 and activated caspase-3) in the fructose-induced metabolic syndrome were significantly increased compared with the non-metabolic syndrome. (5) Cardiac IGFI-related survival proteins (IGFI, IGFI-R, p-PI3K and p-Akt) and Bcl-2 family–associated pro-survival proteins (Bcl-2 and Bcl-xL) in the fructose-induced metabolic syndrome were significantly decreased compared with the non-metabolic syndrome. After integrating our current findings into previously proposed theories, a hypothesized diagram is drawn in Figure 6, which suggests that cardiac Fas receptor-dependent and mitochondria-dependent pathways were increased, whereas cardiac IGFI-R/PI3K/Akt survival and Bcl-2 family associated pro-survival pathways were decreased in the fructose feeding induced metabolic syndrome.

F6

The consumption of fructose has increased, largely because of an increased consumption of soft drinks and many juice beverages containing sucrose (table sugar consists of 50% fructose, 50% glucose) or high-fructose corn syrup (a single can of beverage contains about 42%–55% fructose).[32,33] Dietary high-fructose intake has been suggested to be an important factor contributing to the development of symptoms of metabolic syndrome. Recent evidence suggests that fructose feeding in rats develops the features of the metabolic syndrome model in many of the same pathophysiological deficits as noted in metabolic syndrome humans, such as insulin resistance, weight gain, hyperlipidemia, hyperinsulinemia, hypertriacylglycerolemia, impaired glucose tolerance, hypertension, myocardial functional abnormalities and heart failure.[3,4,31,32,34] In the current study, daily 50% fructose feeding for 13 weeks caused increases in blood pressure, glucose, insulin, triglyceride and cholesterol levels. Furthermore, abnormal myocardial architecture, enlarged interstitial space and increased TUNEL-positive apoptotic cardiac cells were observed in the rat hearts. The physiological parameters and cardiomyopathic changes found in the current animal models may provide one mechanism to clarify how cardiac morphological change occurs in metabolic syndrome humans.

The Fas receptor-dependent apoptotic pathway is mediated by Fas ligand, Fas receptor, TNF-α, TNFR1, FADD and activated caspase-8. The mitochondria-dependent apoptotic pathway is mediated by Bax, Bak, cytochrome *c*, activated caspase-9 and activated caspase-3.[12,13] In the current study, 50% fructose-fed rats appeared to have significantly activated Fas receptor-dependent apoptotic pathway, as evidenced by increases in Fas ligand, Fas receptor, TNF-α, TNFR1, FADD, activated caspase-8 and activated caspase-3 levels in the hearts. Additionally, fructose-fed rats appeared to have a significantly activated mitochondria-dependent apoptotic pathway, as evidenced by increases in the levels of Bax, Bak, Bax/Bcl-2, Bak/Bcl-xL, cytochrome *c*, activated caspase-9 and activated caspase-3 in the hearts. All key components of Fas receptor-dependent and mitochondria-dependent apoptotic pathways, from upstream cascade to downstream cascade, consistently show pro-apoptotic effects in the hearts excised from the fructose-induced metabolic syndrome rats. These are the first data to demonstrate that fructose intake activates the cardiac Fas receptor-dependent and mitochondria-dependent apoptotic pathways, which might lead to cardiac apoptosis.

The IGFI/IGFI-R and their downstream PI3K and Akt signaling pathways have been indicated to contribute to modulation of survival and apoptotic responses in cardiac tissue.[25,35] Our previous study shows decreased IGFI/PI3K/Akt survival pathways via decreases in IGFI, IGFI-R, PI3K and Akt in the diabetic rat heart.[8] In the present study, the cardiac IGFI-related survival signaling was significantly decreased in 50% fructose-fed rats based on decreased IGFI, IGFI-R, p-PI3K and p-Akt levels. The mitochondria-dependent apoptotic pathway is tightly controlled by the Bcl-2 family. Pro-apoptotic and pro-survival members of the Bcl-2 family seem to interact with and neutralize each other so that the relative balance of these effectors strongly influences cell fate.[18,36] Shifting the balance of Bcl-2 family members toward pro-apoptotic effects will activate caspase-9, which further activates caspase-3 and executes the apoptotic program.[19] In the current study, the cardiac pro-survival pathway was significantly decreased in 50% fructose-fed rats based on the decreased Bcl-2 and Bcl-xL levels. Therefore, our findings strongly suggest that

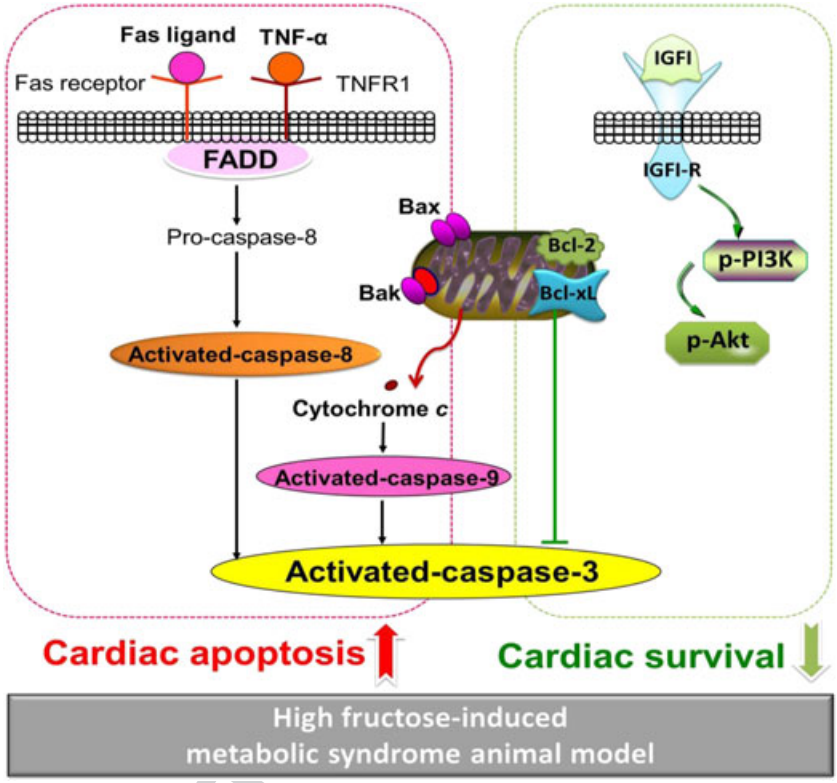

Figure 6. Our proposed hypothesis that the cardiac Fas-dependent and mitochondria-dependent apoptotic pathways will be activated in fructose-induced metabolic syndrome. Evidence is based on high fructose-fed associated increases in Fas-dependent apoptotic pathway (TNF-α, TNFR1, Fas ligand, Fas receptor, FADD, caspase-8 and caspase-3) and the mitochondria-dependent apoptotic pathway (Bax, Bak, cytochrome *c*, caspase-9 and caspase-3). In contrast, the cardiac pro-survival pathways become less activated in the metabolic syndrome animal model. The evidence is based on fructose-fed associated decreases in the survival pathway (IGFI, IGFI-R, p-PI3K, p-Akt, Bcl-2 and Bcl-xL)

the cardiac IGFI-related survival and Bcl-2 family associated pro-survival pathways become less activated in the fructose-induced metabolic syndrome animal model, which might lead to developing cardiac apoptosis and the consequential development of heart failure.

HYPOTHESIZED AND CLINICAL APPLICATION

An increase in fructose intake has been linked with a rise in obesity and metabolic disorders. The current metabolic syndrome animal model under high fructose-feeding proves to be an important representation of metabolic syndrome inducing abnormal myocardial architecture and cardiac apoptosis in metabolic syndrome humans because of cardiac tissues being difficult to sample from human hearts; moreover, high-fructose consumption increased blood pressure, glucose, insulin, triglyceride and cholesterol levels. Previous studies indicated that obesity and hypertension enhanced cardiac Fas-dependent and mitochondria-dependent apoptotic pathways,[9,10,23,24] and streptozotocin-induced diabetes activated cardiac mitochondria-dependent apoptotic pathways in rat models.[8,35] Overall, our current findings indicate that the activation of cardiac Fas-dependent and mitochondria-dependent apoptotic pathways, as well as the cardiac IGFI/PI3K/Akt survival pathway being suppressed in fructose-induced metabolic syndrome rats, might provide an important mechanism in the explanation of the development of cardiomyopathy. Furthermore, additional questions will be raised, such as whether anti-apoptotic therapy might be beneficial to attenuate cardiac Fas-dependent and/or mitochondria-dependent apoptotic pathways when considering possible therapeutic agents to control or prevent the development of apoptosis-related cardiac diseases in metabolic syndrome. Of course, further therapeutic and clinical studies are required to clarify the effects of treatments or the survival and apoptotic mechanisms in metabolic syndrome-related heart diseases.

CONFLICT OF INTEREST

The authors have declared that there is no conflict of interest.

ACKNOWLEDGMENT

This study was supported by grants from the National Science Council (NSC 99-2410-H-468-030-MY3 and 98-2314-B-040-001-MY3) and the China Medical University and Asia University (CMU99-ASIA-05) in Taiwan. This study is supported in part by Taiwan Department of Health Clinical Trial and Research Center of Excellence (DOH101-TD-B-111-004). The pathway diagram in the current study was modified from the Pathway Central from SABiosciences.

REFERENCES

1. Reaven GM. Banting lecture 1988. Role of insulin resistance in human disease. *Diabetes* 1988; **37**: 1595–1607.
2. Isomaa B, Almgren P, Tuomi T, *et al*. Cardiovascular morbidity and mortality associated with the metabolic syndrome. *Diabetes Care* 2001; **24**: 683–689.
3. Mottillo S, Filion KB, Genest J, *et al*. The metabolic syndrome and cardiovascular risk a systematic review and meta-analysis. *J Am Coll Cardiol* 2010; **56**: 1113–1132.
4. Malik S, Wong ND, Franklin SS, *et al*. Impact of the metabolic syndrome on mortality from coronary heart disease, cardiovascular disease, and all causes in United States adults. *Circulation* 2004; **110**: 1245–1250.
5. Nisoli E, Clementi E, Carruba MO, Moncada S. Defective mitochondrial biogenesis: a hallmark of the high cardiovascular risk in the metabolic syndrome? *Circ Res* 2007; **100**: 795–806.
6. Narula J, Pandey P, Arbustini E, *et al*. Apoptosis in heart failure: release of cytochrome c from mitochondria and activation of caspase-3 in human cardiomyopathy. *Proc Natl Acad Sci USA* 1999; **96**: 8144–8149.
7. Boudina S, Abel ED. Mitochondrial uncoupling: a key contributor to reduced cardiac efficiency in diabetes. *Physiology (Bethesda)* 2006; **21**: 250–258.
8. Cheng SM, Ho TJ, Yang AL, *et al*. Exercise training enhances cardiac IGFI-R/PI3K/Akt and Bcl-2 family associated pro-survival pathways in streptozotocin-induced diabetic rats. *Int J Cardiol* 2012. doi:10.1016/j.ijcard.2012.01.031.
9. Lee SD, Shyu WC, Cheng IS, *et al*. Effects of exercise training on cardiac apoptosis in obese rats. *Nutr Metab Cardiovasc Dis* 2012. doi:10.1016/j.numecd.2011.11.002.
10. Huang CY, Yang AL, Lin YM, *et al*. Anti-apoptotic and pro-survival effects of exercise training on hypertensive hearts. *J Appl Physiol* 2012; **112**: 883–891.
11. Lee SD, Chu CH, Huang EJ, *et al*. Roles of insulin-like growth factor II in cardiomyoblast apoptosis and in hypertensive rat heart with abdominal aorta ligation. *Am J Physiol Endocrinol Metab* 2006; **291**: E306–E314.
12. Haunstetter A, Izumo S. Apoptosis: basic mechanisms and implications for cardiovascular disease. *Circ Res* 1998; **82**: 1111–1129.
13. Bishopric NH, Andreka P, Slepak T, Webster KA. Molecular mechanisms of apoptosis in the cardiac myocyte. *Curr Opin Pharmacol* 2001; **1**: 141–150.
14. Barnhart BC, Alappat EC, Peter ME. The CD95 type I/type II model. *Semin Immunol* 2003; **15**: 185–193.
15. Bang S, Jeong EJ, Kim IK, Jung YK, Kim KS. Fas- and tumor necrosis factor-mediated apoptosis uses the same binding surface of FADD to trigger signal transduction. A typical model for convergent signal transduction. *J Biol Chem* 2000; **275**: 36217–36222.
16. Jeremias I, Stahnke K, Debatin KM. CD95/Apo-1/Fas: independent cell death induced by doxorubicin in normal cultured cardiomyocytes. *Cancer Immunol Immunother* 2005; **54**: 655–662.
17. Adams JM, Cory S. Life-or-death decisions by the Bcl-2 protein family. *Trends Biochem Sci* 2001; **26**: 61–66.
18. Kubasiak LA, Hernandez OM, Bishopric NH, Webster KA. Hypoxia and acidosis activate cardiac myocyte death through the Bcl-2 family protein BNIP3. *Proc Natl Acad Sci USA* 2002; **99**: 12825–12830.
19. Brown GC, Borutaite V. Nitric oxide, cytochrome c and mitochondria. *Biochem Soc Symp* 1999; **66**: 17–25.
20. Lee SD, Kuo WW, Lin JA, *et al*. Effects of long-term intermittent hypoxia on mitochondrial and Fas death receptor dependent apoptotic pathways in rat hearts. *Int J Cardiol* 2007; **116**: 348–356.
21. Lee SD, Kuo WW, Wu CH, *et al*. Effects of short- and long-term hypobaric hypoxia on Bcl2 family in rat heart. *Int J Cardiol* 2006; **108**: 376–384.
22. Lee SD, Kuo WW, Lin JA, *et al*. Effects of long-term intermittent hypoxia on mitochondrial and Fas death receptor dependent apoptotic pathways in rat hearts. *Int J Cardiol* 2007; **116**: 348–356.
23. Lee SD, Tzang BS, Kuo WW, *et al*. Cardiac fas receptor-dependent apoptotic pathway in obese Zucker rats. *Obesity (Silver Spring)* 2007; **15**: 2407–2415.
24. Lu MC, Tzang BS, Kuo WW, *et al*. More activated cardiac mitochondrial-dependent apoptotic pathway in obese Zucker rats. *Obesity Silver Spring, Md* 2007; **15**: 2634–2642.
25. Sun HY, Zhao RR, Zhi JM. Insulin-like growth factor I inhibits cardiomyocyte apoptosis and the underlying signal transduction pathways. *Methods Find Exp Clin Pharmacol* 2000; **22**: 601–607.
26. Hong F, Kwon SJ, Jhun BS, *et al*. Insulin-like growth factor-1 protects H9c2 cardiac myoblasts from oxidative stress-induced apoptosis via phosphatidylinositol 3-kinase and extracellular signal-regulated kinase pathways. *Life Sci* 2001; **68**: 1095–1105.
27. Ren J, Samson WK, Sowers JR. Insulin-like growth factor I as a cardiac hormone: physiological and pathophysiological implications in heart disease. *J Mol Cell Cardiol* 1999; **31**: 2049–2061.
28. Vincent AM, Feldman EL. Control of cell survival by IGF signaling pathways. *Growth Horm IGF Res* 2002; **12**: 193–197.
29. Matsui T, Davidoff AJ. Assessment of PI-3 kinase and Akt in ischemic heart diseases in diabetes. *Methods Mol Med* 2007; **139**: 329–338.
30. Liu X, Kim CN, Yang J, Jemmerson R, Wang X. Induction of apoptotic program in cell-free extracts: requirement for dATP and cytochrome c. *Cell* 1996; **86**: 147–157.
31. Hwang IS, Ho H, Hoffman BB, Reaven GM. Fructose-induced insulin resistance and hypertension in rats. *Hypertension* 1987; **10**: 512–516.
32. Rutledge AC, Adeli K. Fructose and the metabolic syndrome: pathophysiology and molecular mechanisms. *Nutr Rev* 2007; **65**: S13–S23.
33. Tappy L, Le KA TC, Paquot N. Fructose and metabolic diseases: new findings, new questions. *Nutrition Burbank, Los Angeles County, Calif* 2010; **26**: 1044–1049.
34. Ren J, Pulakat L, Whaley-Connell A, Sowers JR. Mitochondrial biogenesis in the metabolic syndrome and cardiovascular disease. *J Mol Med (Berlin, Germany)* 2010; **88**: 993–1001.
35. Kuo WW, Chung LC, Liu CT, *et al*. Effects of insulin replacement on cardiac apoptotic and survival pathways in streptozotocin-induced diabetic rats. *Cell Biochem Funct* 2009; **27**: 479–487.
36. McGowan BS, Ciccimaro EF, Chan TO, Feldman AM. The balance between pro-apoptotic and anti-apoptotic pathways in the failing myocardium. *Cardiovasc Toxicol* 2003; **3**: 191–206.

WILEY-BLACKWELL

USING e-ANNOTATION TOOLS FOR ELECTRONIC PROOF CORRECTION

Required software to e-Annotate PDFs: Adobe Acrobat Professional or Adobe Reader (version 7.0 or above). (Note that this document uses screenshots from Adobe Reader X)
The latest version of Acrobat Reader can be downloaded for free at: http://get.adobe.com/uk/reader/

Once you have Acrobat Reader open on your computer, click on the Comment tab at the right of the toolbar:

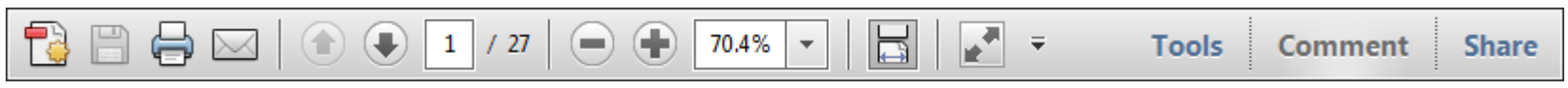

This will open up a panel down the right side of the document. The majority of tools you will use for annotating your proof will be in the Annotations section, pictured opposite. We've picked out some of these tools below:

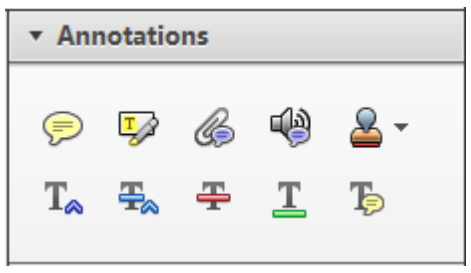

1. Replace (Ins) Tool – for replacing text.

Strikes a line through text and opens up a text box where replacement text can be entered.

How to use it

- Highlight a word or sentence.
- Click on the Replace (Ins) icon in the Annotations section.
- Type the replacement text into the blue box that appears.

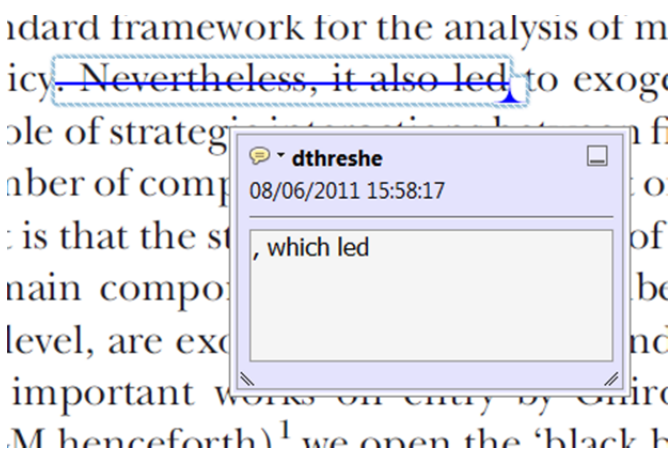

2. Strikethrough (Del) Tool – for deleting text.

Strikes a red line through text that is to be deleted.

How to use it

- Highlight a word or sentence.
- Click on the Strikethrough (Del) icon in the Annotations section.

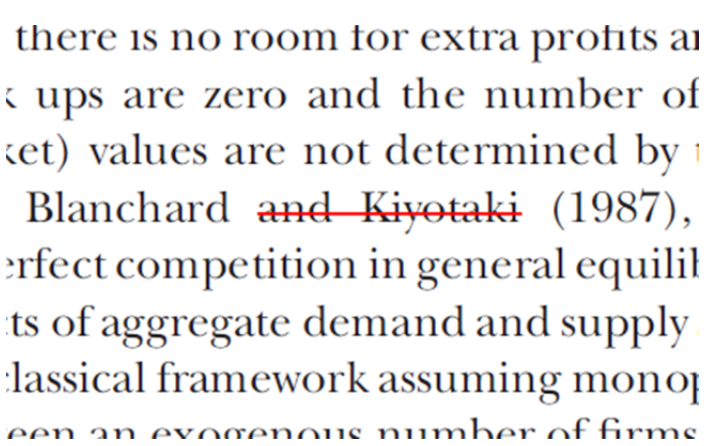

3. Add note to text Tool – for highlighting a section to be changed to bold or italic.

Highlights text in yellow and opens up a text box where comments can be entered.

How to use it

- Highlight the relevant section of text.
- Click on the Add note to text icon in the Annotations section.
- Type instruction on what should be changed regarding the text into the yellow box that appears.

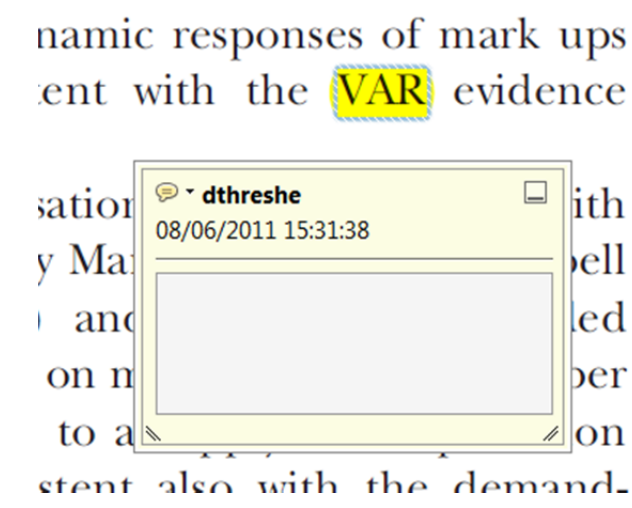

4. Add sticky note Tool – for making notes at specific points in the text.

Marks a point in the proof where a comment needs to be highlighted.

How to use it

- Click on the Add sticky note icon in the Annotations section.
- Click at the point in the proof where the comment should be inserted.
- Type the comment into the yellow box that appears.

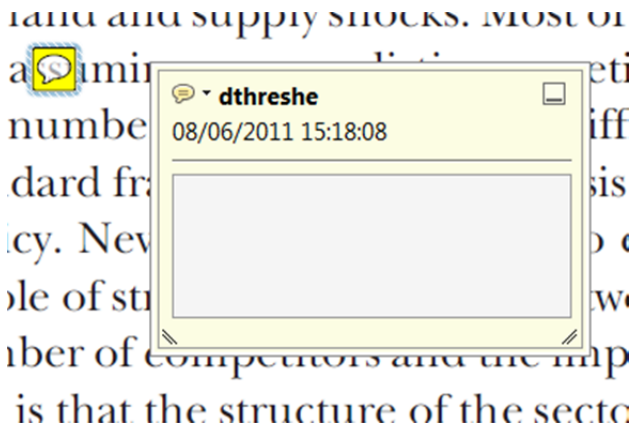

WILEY-BLACKWELL

USING e-ANNOTATION TOOLS FOR ELECTRONIC PROOF CORRECTION

5. Attach File Tool – for inserting large amounts of text or replacement figures.

Inserts an icon linking to the attached file in the appropriate pace in the text.

How to use it

- Click on the Attach File icon in the Annotations section.
- Click on the proof to where you'd like the attached file to be linked.
- Select the file to be attached from your computer or network.
- Select the colour and type of icon that will appear in the proof. Click OK.

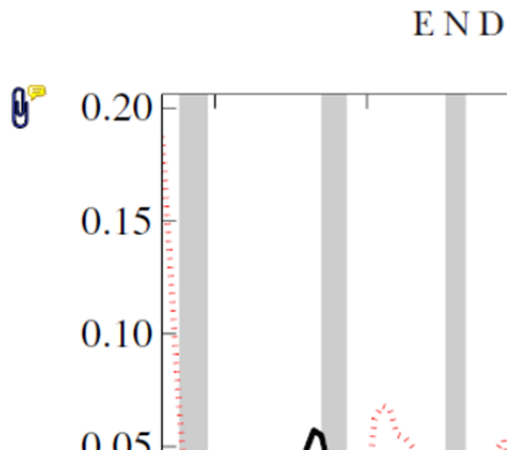

6. Add stamp Tool – for approving a proof if no corrections are required.

Inserts a selected stamp onto an appropriate place in the proof.

How to use it

- Click on the Add stamp icon in the Annotations section.
- Select the stamp you want to use. (The Approved stamp is usually available directly in the menu that appears).
- Click on the proof where you'd like the stamp to appear. (Where a proof is to be approved as it is, this would normally be on the first page).

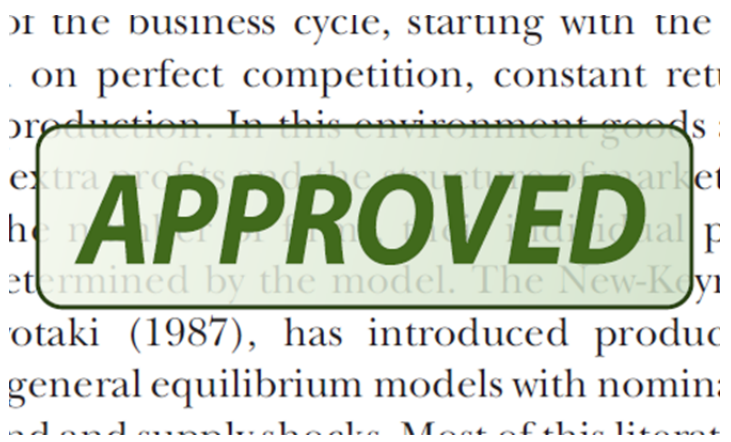

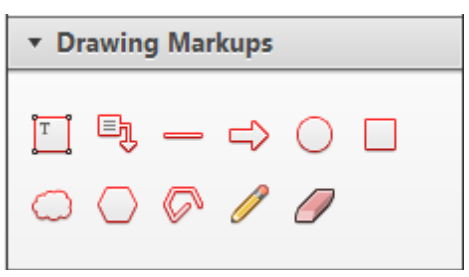

7. Drawing Markups Tools – for drawing shapes, lines and freeform annotations on proofs and commenting on these marks.

Allows shapes, lines and freeform annotations to be drawn on proofs and for comment to be made on these marks..

How to use it

- Click on one of the shapes in the Drawing Markups section.
- Click on the proof at the relevant point and draw the selected shape with the cursor.
- To add a comment to the drawn shape, move the cursor over the shape until an arrowhead appears.
- Double click on the shape and type any text in the red box that appears.

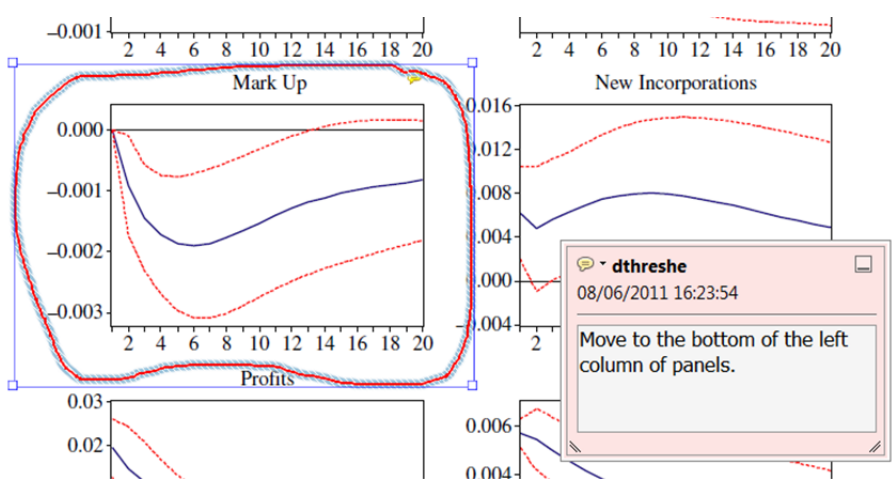

For further information on how to annotate proofs, click on the Help menu to reveal a list of further options:

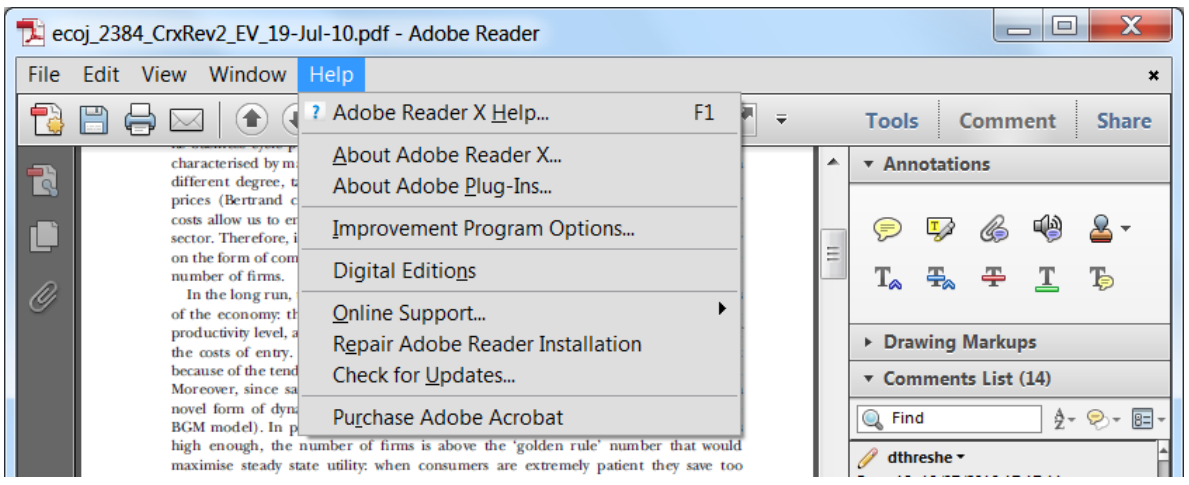

2012 年在 Boston Downtown 的美國睡眠醫學會年會自 6 月 9 日至 6 月 13 日一連舉行五天，前兩天為 postgraduate 的研習會，我參加 year-In-Review 2012 與睡眠呼吸障礙的處置，前面的討論會對過去一整年的文獻作回顧，有許多令人驚艷的論文發表，其中包括睡眠呼吸障礙在高危險妊娠與對孩童行為的障礙的角色，如：過動症與注意力不集中，另外亦討論到睡眠不足的人與日間清醒的能力，在人與動物方面的研究，又由功能性腦波圖的紀錄與分析，睡眠剝奪的人與動物，一為非侵襲，一為侵襲的檢查，可以發現縱然外觀表現張眼的清醒態，事實上大腦多處皮質仍不時有徐動波出現，這說明一個缺乏睡眠的大腦，在專注力缺失，或無法對事情的清楚判定或理解，原因是其來有自的。那就是，不定時、不定區腦部細胞的疲乏，與難以整合可以明顯反應出為何值班與輪班人員其理解力、創造力，甚至情緒與行為自制力的缺失，原來就建立在這疲乏嗜睡的大腦，同樣這種大腦的分離亦可能反應於夜眠時刻，及部分腦入睡、部分腦清醒、部分腦位於混沌時刻，這真是令人大開眼界。而在另一主題為如何處理特殊的睡眠呼吸障礙的病患，這些病患包括心臟衰竭合併中樞型睡眠呼吸中止症，鴉片服用之病患，其治療的方式不再是 CPAP 而是 BiPAP,ASV,AVAPS 與 APAP,其中的複雜性相當高，另外部分原理在短短時間內仍無法完全吸收是項遺憾，不過在台灣臨床給付如此低廉的狀態，我真擔心不會有太多醫師願意投注時間在這夜眠時刻，以矯正這群病患的常態性失眠。儘管如此，我亦能對這群特殊病患睡眠呼吸障礙，從病理生理學的角度切入來理解其治療的策略是否有何不同，也許幾年後，上述各種

呼吸器或呼吸輔助器，經由創新與病理生理學的進一步理解，期能改進病患求得一夜好眠的「基本權利」。

另外一項令人印象深刻的討論會，乃針對兒童睡眠醫學的熱門議題，尤其是重要但仍其爭議性的事，其實最明顯地就是兒童在睡眠多項生理檢測中，不若大人的易於驚醒，易於發生呼吸中止或呼吸不足的情形，亦不常有低血氧的現象，臨床上雖僅打鼾，或稍有呼吸不順即可連帶生長遲緩、行為與學習障礙。史丹佛大學有一套較敏感的測試，即加上橫膈肌肌電圖與呼吸圖作「上呼吸道高阻力症候群」的分析，而義大利的一研究團隊利用腦波圖分析「CAP」與腦下交感神經驚醒指數，分析孩童的睡眠品質，說明客觀的睡眠生理指標在孩童的呼吸障礙，仍有一段路要走。儘管如此，目前的標準仍是為全球睡眠醫學學者接受而為共通的議題討論標準。另外討論話題亦涵蓋嬰兒，母親因睡眠呼吸中止而衍生的疾病與死亡的案例，孩童接受全身性麻醉時，睡眠呼吸中止症的影響，與孩童失眠問題如何定義與量化。另外，猝睡症與孩童感染或疫苗注射的時機的關聯性與鐵不足與孩童過動症與不寧腿症的影響。其實五天的課程包羅萬象，從基礎到臨床，從分子細胞到生理心理學反應，一份簡章的報告難以涵蓋其中。

本研究單位亦展示一張這期研究成果海報如下：

Scaling exponent α presents a function of VLF/HF at wakefulness and during different phases of sleep in healthy males: A surrogate of circadian pacemaker on cardiac dynamics at night sleep

Hua Ting[a,b], Ching-Hsiang Lai[c], Ren-Jing Huang[d], Ya-Yun Hsiao[d], Shu-Yun Chang[a], Ai-Hui Chung[a], Shin-Da Lee[f]

[a] Sleep Medicine Center, Chung Shan Medical University Hospital, Taichung, Taiwan
[b] Institute of Medicine, Chung Shan Medical University, Taichung, Taiwan
[c] Department of Applied Information Sciences, Chung Shan Medical University, Taichung, Taiwan
[d] Department of Medical Image and Radiological Sciences, Chung Shan Medical University, Taichung, Taiwan
[f] Department of Physical Therapy, Graduate Institute of Rehabilitation Science, China Medical University, Taichung, Taiwan
Chung Shan Medical University, No. 110, Sec. 1, Jianguo North Road, Taichung 402, Taiwan

ABSTRACT

Objective: Related to irregular geometric objects that display self-similarity, fractal heart rate variability, better than spectral one day and night, offers clinical implications on aging, gender and cardiovascular prognosis. The human scaling exponent α exhibits a significant circadian rhythm. The parasympathetic modulation of heart rate was mostly driven by the circadian system. The thermoregulatory mechanism positively correlates with the circadian rhythm. To examine the hypothesis that α value should be the function of spectral parameters relevant to aforementioned two issues, we conducted mathematical modeling the relation between fractal and spectral characteristics of heart rate variability at wakefulness and various sleep stages in male workers, beyond the age and sleep-disordered-breathing (SDB) concerns.

Method: In a community-based cohort, 94 male sedentary workers (44.1±7.7 yrs, 27.3±3.4 kg/m²), who had various sleep phases and ectopic-free EKG recordings in an overnight polysomnogram without healthy complaints were recruited. All these subjects were subgrouped by whether older (> 45 years of age) or suffered from SDB (apnea hypopnea index >10 events/hour) into A. Junior-nSDB, B. Junior-SDB, C. Senior-nSDB, and D. Senior-SDB. All five-min EKG wavelets, in pre-sleep wakefulness, non-rapid eye movement stage 2 sleep, slow wave sleep, and first and last terms of REM sleeps, were processed by detrended fluctuation analysis; and fast Fourier transform power spectral analyses to get exponent slope α; and powers of high-(HF), low-(LF), and very low-(VLF) frequencies, respectively. To avoid skew distributions and seek for better fitting, the spectral power values should have natural logarithm transformed in correlating with α.

Results: The participants had values of wide spectrum in apnea hypopnea index, arousal index, and O_2 desatuation index (18.8±20.9, 32.9±17.9, and 17.1±17.0 events/hr, respectively). Within four groups, the values of α, ln(HF), ln(LF), and ln(VLF) were quite similar regardless to various stages. As previous studies, α values were highest in two rapid eye movement sleep and wakefulness than Stage 2 (S_2) and slow wave sleeps (SWS) in four groups. Intriguingly, by linear regression analysis in all four groups and all subjects, power values of ln(HF) and ln(VLF), but not ln(LF) had excellent correlation with corresponding α values in five aforementioned stages, where absolute values of ln(VLF) and ln(HF) were almost equal but reversed in signs. The general linear modeling (GLM) results further indicated that grouping, stages, grouping- or stage-interactive power values of ln(HF) and ln(VLF) had no correlation with corresponding α, except ln(HF), ln(VLF) and intercept. Therefore, the mathematical model of all subjects might evolve as:

α = intercept – 0.149 ln(HF) +0.151 ln(VLF) + ε without staging affecting (R^2 = 0.754).

Because the absolute values of constants of ln(HF) and ln(VLF) were almost identical, this model could be simplified further as:

α = intercept + 0.15 ln(VLF/HF) + ε without R^2 change.

Conclusion: The fractal exponent slope α values are positively correlated with the values of ln(VLF/HF) constantly during wakefulness and various sleep stages in male workers without affected by age and SDB. Along with highest values at the first rapid eye movement sleep and lowest at SWS, α values might reflect the surrogate feature for cardiac sympathovagal and neurohumeral balances related to circadian rhythm.

Table 1. The differences of anthropometric characteristics and polysomnographic variables among four subgroups based on ages and severities in sleep disordered breathing (SDB).

	A. age <=45, AHI <=10	B. age <=45, AHI >10	C. age > 45, AHI <=10	D. age > 45, AHI > 10	Overall	P	Scheffe Post Hoc
Total, n	22	25	20	27	94		
Anthropometric characteristics							
Age, yrs	37.5 ± 4.4	38.3 ± 5.7	50.0 ± 4.3	50.7 ± 3.5	44.1 ± 7.7	<0.001	C,D > A,B
BMI, kg/m²	26.3 ± 3.7	29.1 ± 3.9	26.9 ± 2.8	26.9 ± 2.4	27.3 ± 3.4	0.021	B > A
Waist/ Hip Ratio	0.91 ± 0.04	0.93 ± 0.04	0.94 ± 0.05	0.9 ± 0.0	0.9 ± 0.0	0.078	
Life Style							
Smoking Habit, n(%)	11 (50.0)	10 (40.0)	7 (35.0)	16 (59.3)	44 (46.8)	0.110	
Drinking, n(%)	3 (13.6)	5 (20.0)	6 (30.0)	15 (55.6)	29 (30.9)	0.010	D > A
Exercise, n(%)	7 (31.8)	5 (20.0)	13 (65.0)	15 (55.6)	40 (42.6)	0.012	C > B
Blood Pressure							
Pre-sleep Systolic BP, mm Hg	127 ± 10	122 ± 12	126 ± 12	128 ± 13	126 ± 12	0.288	
Pre-sleep Diastolic BP, mm Hg	81 ± 9	78 ± 8	81 ± 8	81 ± 11	80 ± 9	0.411	
Post-sleep Systolic BP, mm Hg	123 ± 12	122 ± 13	124 ± 9	127 ± 14	124 ± 12	0.471	
Post-sleep Diastolic BP, mm Hg	80 ± 8	81 ± 11	81 ± 10	84 ± 11	82 ± 10	0.522	
Variables in PSG							
Total Sleep Time, min	339 ± 56	355 ± 40	354 ± 90	365 ± 52	354 ± 60	0.531	
Sleep Efficiency, %	81 ± 11	82 ± 8	86 ± 7	83 ± 9	83 ± 9	0.280	
Sleep Latency, min	24 ± 19	19 ± 16	12 ± 9	13 ± 11	17 ± 15	0.022	A > C
Latency to REM, min	116 ± 64	117 ± 50	106 ± 54	117 ± 68	114 ± 59	0.926	
Non REM Stage I, %	4.2 ± 2.8	8.7 ± 4.6	4.7 ± 2.8	8.2 ± 4.6	6.6 ± 4.3	<0.001	B,D > A,C
Stage II, %	52.3 ± 9.8	50.3 ± 9.8	56.0 ± 8.6	52.5 ± 7.5	52.6 ± 9.0	0.208	
Stage III+IV, %	14.4 ± 6.9	11.3 ± 8.6	12.3 ± 6.9	9.0 ± 5.7	11.6 ± 7.2	0.074	
REM, %	0.2 ± 0.1	0.2 ± 0.1	0.2 ± 0.1	0.2 ± 0.1	0.2 ± 0.1	0.913	
AHI, events/hr	2.7 ± 2.5	31.7 ± 24.3	4.8 ± 3.1	30.5 ± 18.2	18.8 ± 20.9	<0.001	B,D > A,C
Arousals Index, events/hr	21.1 ± 11.0	39.2 ± 20.4	24.0 ± 11.8	43.1 ± 15.4	32.9 ± 17.9	<0.001	B,D > A,C
Relevent Limb Movement, events/hr	4.3 ± 8.9	5.7 ± 11.3	4.5 ± 10.5	4.7 ± 9.5	4.8 ± 9.9	0.965	
O_2 DI, events/hr	3.3 ± 3.6	30.2 ± 18.6	4.7 ± 3.1	25.4 ± 13.5	17.1 ± 17.0	0.366	
Lowest Oxygen Saturation, %	86.6 ± 6.0	66.9 ± 16.2	79.6 ± 14.0	73.1 ± 8.0	76.0 ± 13.7	<0.001	B,D > A,C
Duration of SaO_2<90% , min	5.7 ± 12.9	55.4 ± 58.5	20.2 ± 62.4	47.2 ± 44.7	33.9 ± 51.8	<0.001	B,D > A

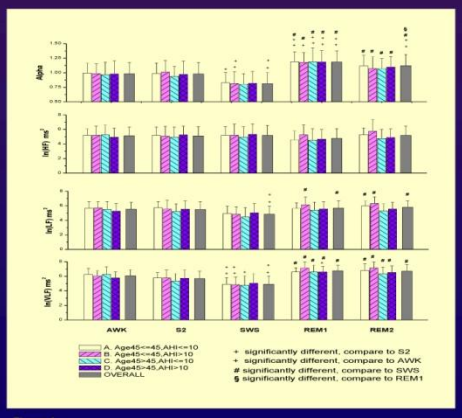

Figure 1
The differences of α values and power values of ln(HF), ln(LF), and ln(VLF) among wakefulness and various sleep stages in four subgroups and overall subjects.

Table 2 . The results of multiple regression analysis for modeling relationship between α values and power values of ln(HF), ln(LF), and/or ln(VLF) among wakefulness and various sleep stages in four subgroups.

Group	independent variable	AWK Beta	AWK P	S2 Beta	S2 P	SWS Beta	SWS P	REM1 Beta	REM1 P	REM2 Beta	REM2 P
A. age <= 45, AHI <= 10	intercept	0.8304	***	0.5218	**	0.8777	***	0.9367	***	0.9284	***
	ln (VLF)	0.1534	***	0.2192	***	0.1623	***	0.1263	***	0.1245	***
	ln (HF)	-0.1534	***	-0.1546	***	-0.1623	***	-0.1263	***	-0.1245	***
B. age <= 45, AHI > 10	intercept	0.8776	***	0.8988	***	0.8733	***	0.5696	**	0.8760	***
	ln (VLF)	0.1267	***	0.1606	***	0.1636	***	0.1835	***	0.1414	***
	ln (HF)	-0.1267	***	-0.1606	***	-0.1636	***	-0.1336	***	-0.1414	***
C. age > 45, AHI <= 10	intercept	0.8214	***	0.8773	***	1.0930	***	0.8326	***	0.8686	***
	ln (VLF)	0.1455	***	0.1437	***	0.0996	**	0.1704	***	0.1276	***
	ln (HF)	-0.1455	***	-0.1437	***	-0.1547	***	-0.1704	***	-0.1276	***
D. age > 45, AHI > 10	intercept	0.8701	***	0.8872	***	0.8595	***	0.8984	***	0.8952	***
	ln (VLF)	0.1335	***	0.1762	***	0.1558	***	0.1488	***	0.1393	***
	ln (HF)	-0.1335	***	-0.1762	***	-0.1558	***	-0.1488	***	-0.1393	***
Overall	intercept	0.8557	***	0.8892	***	0.9668	***	0.9049	***	0.8923	***
	ln (VLF)	0.1365	***	0.1620	***	0.1391	***	0.1423	***	0.1337	***
	ln (HF)	-0.1365	***	-0.1620	***	-0.1606	***	-0.1423	***	-0.1337	***

Table 3. The results of multiple regression analysis for modeling relationship between α values and power values of ln(HF), ln(LF), and/or ln(VLF) among wakefulness and various sleep stages in overall subjects.

Source	SS	df	MS	F	p
intercept	6.710	1	6.710	550.349	0.000
group	0.054	3	0.018	1.463	0.224
stage	0.076	4	0.019	1.560	0.184
ln(HF)	10.236	1	10.236	839.528	0.000
ln(VLF)	5.560	1	5.560	456.021	0.000
Group * ln(HF)	0.034	3	0.011	0.941	0.421
Group * ln(VLF)	0.026	3	0.009	0.700	0.553
stage * ln(HF)	0.063	4	0.016	1.283	0.276
stage * ln(VLF)	0.085	4	0.021	1.734	0.141
Error	5.438	446	0.012		

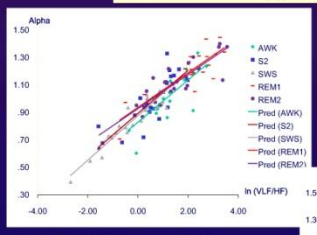

Figure 2. The individual regression line between power values of ln(VLF/HF) and corresponding α values at wakefulness or various sleep stages in subgroup A (A. Junior-nSDB).

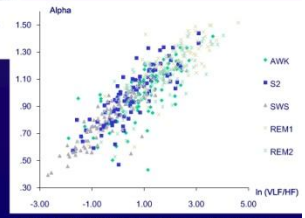

Figure 3. The relationship between power values of ln(VLF/HF) and corresponding α values at wakefulness and various sleep stages in overall subjects.

國科會補助計畫衍生研發成果推廣資料表

日期:2013/05/30

國科會補助計畫	計畫名稱: 內皮素A型受體拮抗劑配合運動治療對睡眠呼吸終止症誘發心臟細胞凋亡的療效探討
	計畫主持人: 丁化
	計畫編號: 98-2314-B-040-001-MY3　　學門領域: 復健科

無研發成果推廣資料

98 年度專題研究計畫研究成果彙整表

計畫主持人：丁化	計畫編號：98-2314-B-040-001-MY3
計畫名稱：內皮素 A 型受體拮抗劑配合運動治療對睡眠呼吸終止症誘發心臟細胞凋亡的療效探討	

成果項目			量化			單位	備註（質化說明：如數個計畫共同成果、成果列為該期刊之封面故事...等）
			實際已達成數（被接受或已發表）	預期總達成數(含實際已達成數)	本計畫實際貢獻百分比		
國內	論文著作	期刊論文	0	0	100%	篇	
		研究報告/技術報告	0	0	100%		
		研討會論文	0	0	100%		
		專書	0	0	100%		
	專利	申請中件數	0	0	100%	件	
		已獲得件數	0	0	100%		
	技術移轉	件數	0	0	100%	件	
		權利金	0	0	100%	千元	
	參與計畫人力（本國籍）	碩士生	0	0	100%	人次	
		博士生	0	0	100%		
		博士後研究員	0	0	100%		
		專任助理	0	0	100%		
國外	論文著作	期刊論文	1	3	100%	篇	
		研究報告/技術報告	0	0	100%		
		研討會論文	0	0	100%		
		專書	0	0	100%	章/本	
	專利	申請中件數	0	0	100%	件	
		已獲得件數	0	0	100%		
	技術移轉	件數	0	0	100%	件	
		權利金	0	0	100%	千元	
	參與計畫人力（外國籍）	碩士生	0	0	100%	人次	
		博士生	0	0	100%		
		博士後研究員	0	0	100%		
		專任助理	0	0	100%		

其他成果 (無法以量化表達之成果如辦理學術活動、獲得獎項、重要國際合作、研究成果國際影響力及其他協助產業技術發展之具體效益事項等，請以文字敘述填列。)	無

	成果項目	量化	名稱或內容性質簡述
科教處計畫加填項目	測驗工具(含質性與量性)	0	
	課程/模組	0	
	電腦及網路系統或工具	0	
	教材	0	
	舉辦之活動/競賽	0	
	研討會/工作坊	0	
	電子報、網站	0	
	計畫成果推廣之參與（閱聽）人數	0	

國科會補助專題研究計畫成果報告自評表

請就研究內容與原計畫相符程度、達成預期目標情況、研究成果之學術或應用價值（簡要敘述成果所代表之意義、價值、影響或進一步發展之可能性）、是否適合在學術期刊發表或申請專利、主要發現或其他有關價值等，作一綜合評估。

1. 請就研究內容與原計畫相符程度、達成預期目標情況作一綜合評估
   □達成目標
   ■未達成目標（請說明，以 100 字為限）
      □實驗失敗
      □因故實驗中斷
      ■其他原因
   說明：
   施打內皮素 A 型受體拮抗劑似乎有毒性, 調整方向, 可發表

2. 研究成果在學術期刊發表或申請專利等情形：
   論文：■已發表 □未發表之文稿 □撰寫中 □無
   專利：□已獲得 □申請中 ■無
   技轉：□已技轉 □洽談中 ■無
   其他：(以 100 字為限)

3. 請依學術成就、技術創新、社會影響等方面，評估研究成果之學術或應用價值（簡要敘述成果所代表之意義、價值、影響或進一步發展之可能性）(以 500 字為限)
   提供預防傷害機轉